TIME-DEPENDENT BURGERS-ROTT VORTEX
AS SEEN BY A SIMULATED DOPPLER RADAR

Vincent T. Wood, Robert P. Davies-Jones, and Rodger A. Brown
National Severe Storms Laboratory, Norman, Oklahoma

1.   INTRODUCTION

Brown et al. (1978, 2002) discussed important characteristics of the tornadic vortex signature (TVS), which occurs when the diameter of a Doppler radar beam is larger than or equal to a tornado vortex. The TVS is a Doppler velocity signature of large shear, coincident with the tornado-scale circulation, characterized by Doppler velocity maxima of opposite signs approximately one beamwidth apart. Not all tornadoes produce identifiable signatures because TVS detection is a function of tornado core diameter and strength as well as the size of the radar sampling volume.

It is not clear how the TVS behaves as it corresponds to different stages of tornado evolution. One cannot determine whether the time-varying TVS is due to changes in tornado intensity/size, due to the location of the tornado relative to the size and spatial distribution of the radar pulse volumes (Brown et al. 1978, 2002; Burgess et al. 1993; Wood and Brown 1997), due to differential power weighting of the velocity spectrum in regions of strong reflectivity gradients (Bluestein et al. 1993), or due to centrifugal action on hydrometers and debris by the tornado (Wurman and Gill 2000; Dowell et al. 2001). Burgess et al. (2002) compared high-resolution DOW (Doppler On Wheels) radar data to lower-resolution WSR-88D (Weather Surveillance Radar-88 Doppler) observations of the 3 May 1999 Oklahoma City tornado. They concluded that the strength of the WSR-88D signature was only a rough measure of tornado intensity.

In this paper, we use simulated WSR-88D data as a means for understanding how a simulated TVS behaves during various stages of tornado evolution. The simulations are of a time-dependent version of the Burgers-Rott vortex (henceforth BRV), which is an exact solution of the Navier-Stokes equations of motion and continuity for axisymmetric, viscous flow. The meridional flow is steady, but the core radius decreases and the maximum tangential velocity increases with time. The solution approaches a steady BRV asymptotically. Three important parameters in the solution are kinematic viscosity, horizontal convergence, and angular momentum at infinity, all of which are independent of height and time. Here we conduct a few experiments with the angular momentum held constant and with different values of horizontal convergence and kinematic viscosity.

2.   BURGERS-ROTT VORTEX

Corresponding author address: Vincent T. Wood, National Severe Storms Laboratory, 1313 Halley Circle, Norman, OK 73069. E-mail: vincent.wood@noaa.gov

The time-dependent version of the Burgers (1948)-Rott (1958) vortex is an exact solution of the Navier-Stokes equations of motion and continuity in cylindrical coordinates (r,ϕ,z) for velocity components (u,v,w) (Rott 1958; Trapp and Davies-Jones 1997) The BRV is embedded in convergent meridional flow. The vortex, centered on the z-axis, has circulation Γ_∞ at radial infinity. The solution is

$$u = -ar , \qquad w = 2az , \qquad (1)$$

and

$$\frac{v(r,t)}{v_m(t)} = \frac{r_c(t)}{0.715 r} \{1 - \exp[-1.257 r^2/r_c^2(t)]\} , \quad (2)$$

where $2a$ is the horizontal convergence. At time t, the core radius of the BRV, $r_c(t)$, and the maximum tangential velocity, $v_m(r,t)$, are given by

$$r_c(t) = [r_c^2(0)\exp(-2at) + r_c^2(\infty)(1 - \exp(-2at)]^{1/2} , \quad (3)$$

$$v_m(t) = 0.715 M_\infty/r_c(t) . \qquad (4)$$

In (3) and (4), $r_c(0)$ is the initial core radius (1 km, arbitrarily) of the vortex at $t = 0$, the core radius at $t = \infty$ is $r_c(\infty) = [1.257(2v_k/a)]^{1/2}$, v_k is the kinematic viscosity, and M_∞ ($\equiv \Gamma_\infty/2\pi$) is the angular momentum at $r = \infty$. The initial state may be regarded as a tornado cyclone. There also is an inviscid solution which is a time-dependent Rankine-combined vortex (RCV). This is given by (1), $r_c(t) = r_c(0)\exp(-at)$, and

$$\frac{v(r,t)}{v_m(t)} = \begin{cases} \dfrac{r}{r_c(t)} , & r \le r_c(t) , \\[2ex] \dfrac{r_c(t)}{r} , & r \ge r_c(t) , \end{cases} \qquad (5)$$

where $v_m(t) = M_\infty/r_c(t) = v_m(0)\exp(at)$ is the maximum tangential velocity. The cusp in the RCV is unrealistic because it would be smoothed out by turbulent diffusion of angular momentum in nature. In both solutions, the normalized tangential velocity $v(r,t)/v_m(t)$ is a function of the normalized radial distance $r/r_c(t)$ alone.

Table 1. The three Burgers-Rott vortices (BRVs) with differing values of horizontal convergence (a) and kinematic viscosity (v_k). The Γ_∞ value is 5 x 10^4 m^2 s^{-1}. Also given are v_m and r_c at $t = \infty$.

Case	a (s^{-1})	v_k (m^2 s^{-1})	$v_m(\infty)$ (m s^{-1})	$r_c(\infty)$ (m)
EXP I	5x10^{-3}	10	80	71
EXP II	10x10^{-3}	10	114	50
EXP III	5x10^{-3}	5	114	50

The three experiments selected for this paper are shown in Table 1. We use the value of Γ_∞ that was observed for the Cleveland tornado (Lewis and Perkins 1953).

Figure 1 shows the time-varying plots of $v_m(t)$ and $r_c(t)$ for the three experiments. The vortices simulate tornadogenesis without a dynamic pipe effect (Trapp and Davies-Jones 1997) because they grow rapidly and form simultaneously at all heights instead of descending slowly from aloft. Provided that $r_c^2(0) >> r_c^2(\infty)$, the initial growth rate of $v_m(t)$ and $r_c^{-1}(t)$ is a (as for the time-dependent RCV). During the developing stage of a BRV, inward advection of angular momentum is much larger than outward diffusion of angular momentum. Consequently, the core contracts and the maximum tangential velocity increases initially with little retardation by diffusion. The BRV eventually reaches a mature, almost steady stage, where advection and diffusion of angular momentum nearly balance. The asymptotic values of $v_m(t)$ and $r_c^{-1}(t)$ are proportional to $(a/v_k)^{1/2}$. In the next section, we explore how the simulated TVS behaves during these two different stages of BRV evolution.
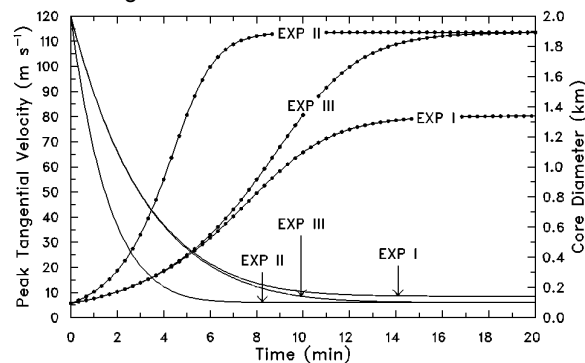
Fig. 1. Peak tangential velocity (dotted curve) and core diameter (solid curve) versus time for the Burgers-Rott vortices (BRVs) of Table 1.

3.   DOPPLER RADAR SIMULATION

The analytical simulation of a WSR-88D, developed by Wood and Brown (1997), was used to produce simulated time-varying velocity measurements from the time-dependent version of the BRV centered at various ranges from the radar. Recall that the rotational velocity field of the BRV is uniform with height. For the simulations, it is assumed that the radar beam pattern is Gaussian shaped. Since it is not clear how the horizontal profile of reflectivity across a tornado vortex varies with height and stage of tornado evolution, a uniform profile of reflectivity is used for the sake of simplicity.

Simulation of the radar sampling process does not directly follow that of a real radar. Instead of averaging radar pulses to produce a simulated mean Doppler velocity value, mean Doppler velocity at the center range and azimuth of the effective resolution volume of the radar beam is obtained by averaging the Doppler velocity component of the BRV solution across the effective radar beam and range-gate depth of 250 m. Two azimuthal sampling intervals (0.5° and 1.0°) corresponding to the

effective beamwidths (1.02° and 1.39°, respectively) are used to compare the magnitudes of the Doppler velocity signature of the BRV. A radar antenna rotating relative to the sampling time produces an effectively broadened beamwidth (Zrnic and Doviak 1976; Doviak and Zrnic 1993). Wood et al. (2001) and Brown et al. (2002) showed that stronger Doppler velocity signatures of mesocyclones and tornadoes typically are produced when the azimuthal sampling interval, and thus the effective beamwidth, is decreased.
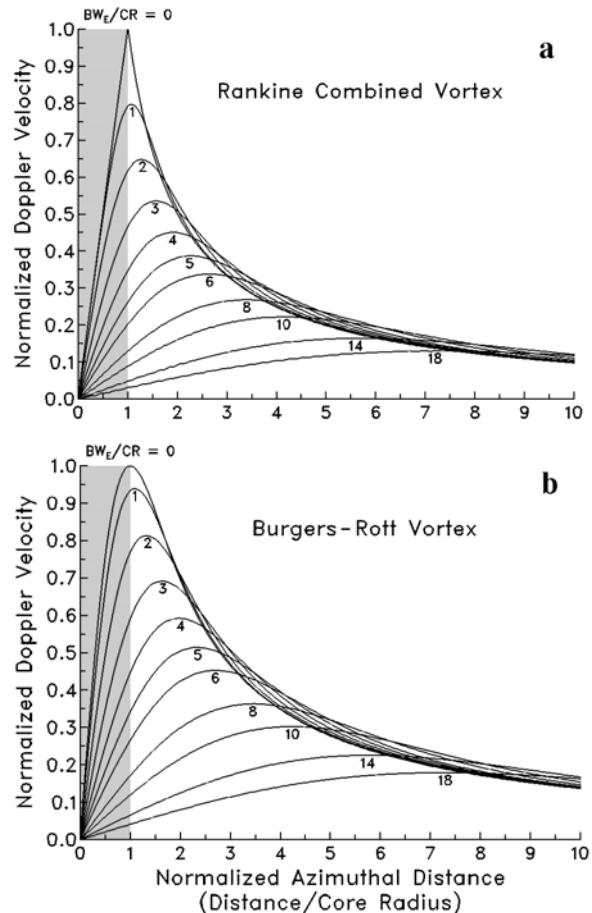
Fig. 2. Continuous velocity profiles across the (a) RCV and (b) BRV for a number of effective beamwidth (BW$_E$) to core radius (CR) ratios. The profiles are normalized. Shaded column represents the core radius of the vortex.

Figure 2 illustrates the continuous velocity profiles across the RCV and BRV for a number of effective beamwidth to core radius ratios. The curves represent the Doppler-velocity azimuthal profiles if the radar were able to make measurements in a continuous manner across the vortex. When the beamwidth is infinitesimally small (i.e., BW$_E$/CR = 0), the profiles are those of the respective vortices. As BW$_E$/CR increases, Doppler velocities are degraded owing to the widening of the beam with range relative to vortex size. Also, the cusp in the RCV profile is smoothed out. At finite beamwidth, the maximum Doppler velocity is reduced more in the case of the RCV because the actual profile has a cusp instead of a rounded peak.

Due to space limitations, we describe only one experiment (EXP I) in detail. The diameter and magnitude of the Doppler vortex signature as functions of time are shown in Fig. 3 for effective beamwidths of 1.39° and 1.02° and ranges of 25 and 50 km from the radar. The magnitude of the signature, ΔV_D, is the velocity difference between the extreme positive and negative Doppler velocity values in the continuous azimuthal profiles around the range circle through the vortex; signature diameter, CD_D, is the distance between these extreme values.
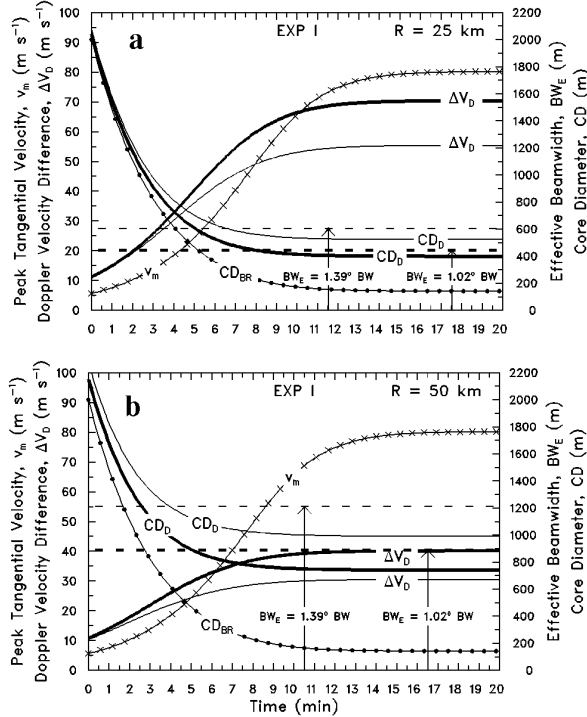
Fig. 3. The velocity difference $\Delta V_D(t)$ and diameter $CD_D(t)$ of the Doppler signature versus time for 1.02° (thick solid line) and 1.39° (thin solid line) effective beamwidths (BW_E) at (a) 25 and (b) 50 km from the radar. Also shown is the time-dependent BRV's maximum tangential velocity $v_m(t)$ (crossed curve) and core diameter [dotted curve, $CD_{BR}(t) = 2r_c(t)$]. The thick (thin) solid horizontal dashed lines indicate the effective beamwidth in m of the 1.02° (1.39°) beams.

At t=0, the BRV is quite well resolved; hence $\Delta V_D(0) \approx 2v_m(0)$ and $CD_D(0) \approx CD_{BR}(0)$ (Fig. 3). Initially, the curve for $v_m(t)$ increases and that for $r_c(t)$ decreases exponentially as in the RCV solution. With time, these curves level out as they approach their asymptotic values. After a few minutes, the Doppler velocity signature becomes a tornadic vortex signature (TVS) as the core diameter of the BRV becomes smaller than the effective beamwidth. Owing to the increased effective beamwidth with range (Fig. 2b), the curves for $\Delta V_D(t)$ and $CD_D(t)$ level out more rapidly than their BRV counterparts to values much less than $2v_m(\infty)$ and much greater than $2r_c(\infty)$, respectively. The underestimation of vortex strength and overestimation of its size increases with

range and effective beamwidth.

Brown et al. (2002) showed that stronger signatures are produced by smaller effective beamwidths. However, Fig. 3 reveals that another advantage of a smaller effective beamwidth is a stronger signature that occurs *earlier*.

Davies-Jones and Stumpf (1997) advocated using circulation in addition to velocity difference for detecting tornadoes and estimating their strengths. Circulation of the Doppler signature, defined here as

$$\Gamma_D(t) = \frac{\pi}{2}\Delta V_D(t)CD_D(t), \qquad (6)$$

is compared in Fig. 4 with the circulation of the BRV outside the core. The latter varies from 3.6 x 10^4 m^2 s^{-1} at the radius of maximum winds to 5 x 10^4 m^2 s^{-1} at radial infinity. The time-varying measured circulations are good estimates of the BRV circulations and are relatively insensitive to range and beamwidth, even after the signatures become TVSs.
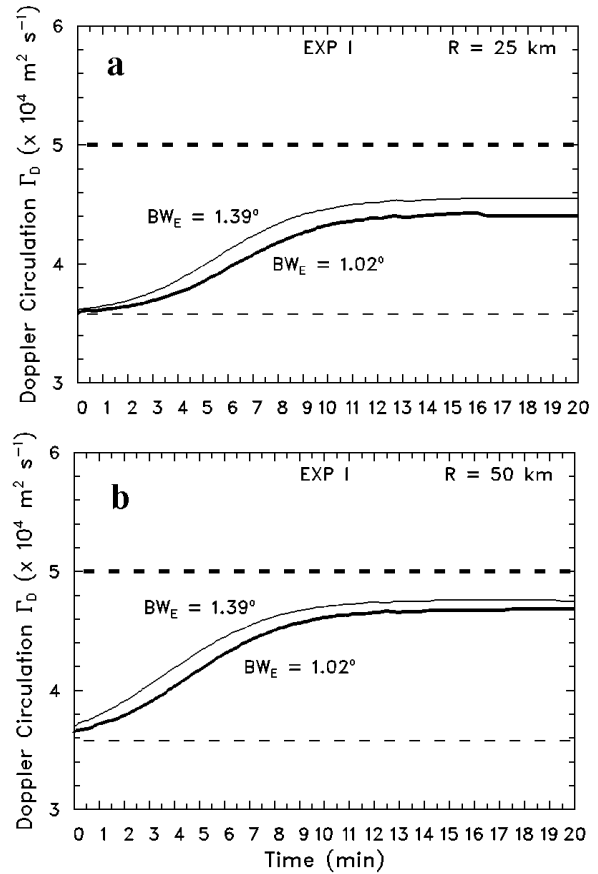
Fig. 4. Signature circulation versus time for the BRV of EXP I and for effective beamwidths of 1.02 (heavy curve) and 1.39 (light curve). Range from the radar is (a) 25 and (b) 50 km. The heavy and light horizontal dashes, respectively, indicate the circulation of the BRV at radial infinity and at the radius of maximum winds.

4. SUMMARY

Simulated WSR-88D measurements of an evolving

Burgers-Rott vortex are presented to understand how a vortex signature varies during the developing and mature stages of a tornado. The results illustrate that signatures are stronger for smaller effective beamwidths. From an operational perspective, TVSs occur earlier with a smaller effective beamwidth. Thus, use of a smaller effective beamwidth than currently used should improve the lead time of tornado warnings and could also result in better detection of weak tornadoes. Signature circulation should be used in addition to velocity difference because it gives good estimates of the circulations of tornadic vortices with relatively little sensitivity to range and beamwidth.

Results are similar for EXP II and III, except that these more intense BRVs are sampled less well owing to their smaller size. The vortex in EXP II forms the most rapidly, and would have the least advance warning between TVS detection and tornado touchdown.

5. FUTURE RESEARCH

One drawback of the present simulations is the assumption of uniform reflectivity across the vortex. Future plans include simulations of nonuniform reflectivity across the BRV, including centrifuging of debris and hydrometers by the vortex.

This paper discusses simulated evolutions of the Burgers-Rott tornadoes. We next will be investigating evolution of actual Doppler signatures of real tornadoes. We collected excellent Archive Level I time series data of the Oklahoma City, Oklahoma supercell tornadic storms of 8-9 May 2003, using the NSSL's WSR-88D KOUN test bed radar in Norman. We will convert the data (reflectivity, mean Doppler velocity, spectrum width) into two separate Archive II (meteorological) datasets that have two different effective beamwidths associated with 0.5^o and 1.0^o azimuthal sampling intervals. We will compare the quality of reflectivity features (such as hook echoes) and of Doppler velocity features (such as TVSs and tornado cyclone signatures) as functions of time, range, azimuthal increment (0.5^o vs 1.0^o), and range increment (0.25 vs 1.0 km for reflectivity only). Additionally, we will compute and compare Doppler signature circulations.

6. REFERENCES

Bluestein, H. B., W. P. Unruh, J. G. LaDue, H. Stein, and D. Speheger, 1993: Doppler radar wind spectra of supercell tornadoes. *Mon. Wea. Rev.,* **121,** 2200-2221.

Brown, R. A., D. W. Burgess, and L. R. Lemon, 1978: Tornado detection by pulsed Doppler radar. *Mon. Wea. Rev.,* **106,** 29-38.

_____, V. T. Wood, and D. Sirmans, 2002: Improved tornado detection using simulated and actual WSR-88D data with enhanced resolution. *J. Atmos. Oceanic Technol.,* **19,** 1759-1771.

Burgers, J. M., 1948: A mathematical model illustrating the theory of turbulence. *Adv. Appl. Mech.,* **1,** 197-199.

Burgess, D. W., R. J. Donaldson, Jr., and P. R. Desrochers, 1993: Tornado detection and warning by radar. *The Tornado: Its Structure, Dynamics, Prediction, and Hazards, Geophys. Monogr.,* No. 79, Amer. Geophys. Union, 203-221.

_____, M. A. Magsig, J. Wurman, D. C. Dowell, and Y. Richardson, 2002: Radar observations of the 3 May 1999 Oklahoma City tornado. *Wea. Forecasting,* **17,** 456-471.

Davies-Jones, R., and G. J. Stumpf, 1997: On the detection and measurement of circulation and areal expansion rate with WSR-88D radars. Preprints, *28th Conf. On Radar Meteorology.* Austin, TX, Amer. Meteor. Soc., 313-314.

Doviak, R. J., and D. S. Zrnic, 1993: *Doppler Radar and Weather Observations.* 2nd Ed. Academic Press, 562 pp.

Dowell, D. C., J. Wurman, and L. J. Wicker, 2001. Centrifuging of scatterers in tornadoes. Preprints, *30th Conf. on Radar Meteorology.* Munich, Germany, Amer. Meteor. Soc., 307-309.

Lewis, W., and P. J. Perkins, 1953: Recorded pressure distribution in the outer portion of a tornado vortex. *Mon. Wea. Rev.,* **81,** 379-385.

Rott, N., 1958: On the viscous core of a line vortex. *Z. Angew. Math. Physik,* **96,** 543-553.

Trapp, R. J., and R. Davies-Jones, 1997: Tornado-genesis with and without a dynamic pipe effect. *J. Atmos. Sci.,* **54,** 113-133.

Wood, V. T., and R. A. Brown, 1997: Effects of radar sampling on single-Doppler velocity signatures of mesocyclones and tornadoes. *Wea. Forecasting,* **12,** 928-938.

_____, R. A. Brown, and D. Sirmans, 2001: Technique for improving detection of WSR-88D mesocyclone signatures by increasing angular sampling. *Wea. Forecasting,* **16,** 177-184.

Wurman, J., and S. Gill, 2000: Finescale radar observations of the Dimmitt, Texas (2 June 1995), tornado. *Mon. Wea. Rev.,* **128,** 2135-2164.

Zrnic, D. S., and R. J. Doviak, 1975: Effective antenna pattern of scanning radars. *IEEE Trans. Aerospace Electron. Systems,* **AES-12,** 551-555.